

We are IntechOpen, the world's leading publisher of Open Access books Built by scientists, for scientists

6,900

Open access books available

186,000

International authors and editors

200M

Downloads

Our authors are among the

154

Countries delivered to

TOP 1%

most cited scientists

12.2%

Contributors from top 500 universities



WEB OF SCIENCE™

Selection of our books indexed in the Book Citation Index
in Web of Science™ Core Collection (BKCI)

Interested in publishing with us?
Contact book.department@intechopen.com

Numbers displayed above are based on latest data collected.
For more information visit www.intechopen.com



Study on IoT and Big Data Analysis of 12" 7 nm Advanced Furnace Process Exhaust Gas Leakage

Kuo-Chi Chang, Kai-Chun Chu, Hsiao-Chuan Wang, Yuh-Chung Lin, Tsui-Lien Hsu and Yu-Wen Zhou

Abstract

Modern FAB uses a large number of high-energy processes, including plasma, CVD, and ion implantation. Furnaces are one of the important tools for semiconductor manufacturing. According to the requirements of conversion production management, FAB installed a set of IoT-based research based on 12" 7 nm-level furnaces chip process. Two furnace processing tool measurement points were set up in a 12-inch 7 nm-level factory in Hsinchu Science Park, Taiwan, this is a 24-hour continuous monitoring system, the data obtained every second is sequentially send and stored in the cloud system. This study will be set in the cloud database for big data analysis and decision-making. The lower limit of TEOS, C₂H₄, CO is 0.4, 1.5, 1 ppm. Semiconductor process, so that IoT integration and big data operations can be performed in all processes, this is an important step to promote FAB intelligent production, and also an important contribution to this research.

Keywords: IoT, big data, furnace, exhaust gas, gas leakage, 7 nm chip process

1. FAB advanced furnace process of 12' nm 7 nm

The semiconductor plant investment exceeds 3 billion US dollars, and the basic operating cost per day exceeds 6 million US dollars, although this process is very important, especially in commercial key sizes below 12 nm (**Figure 1**) [1, 2]. However, modern semiconductor manufacturing has five major difficulties, which are summarized in **Table 1**. Semiconductor refers to the material whose conductivity is between conductor and insulator at normal temperature. Semiconductors are used in integrated circuits, consumer electronics, communication systems, photovoltaic power generation, lighting applications, high-power power conversion and other fields. Such as diode is a device made of semiconductor. Whether from the perspective of technology or economic development, the importance of semiconductors is very huge [3, 4]. 5G and artificial intelligence technologies are the main application areas of advanced technology. For example, in 2019, many mobile phone manufacturers launched 5G models, and most of these models used

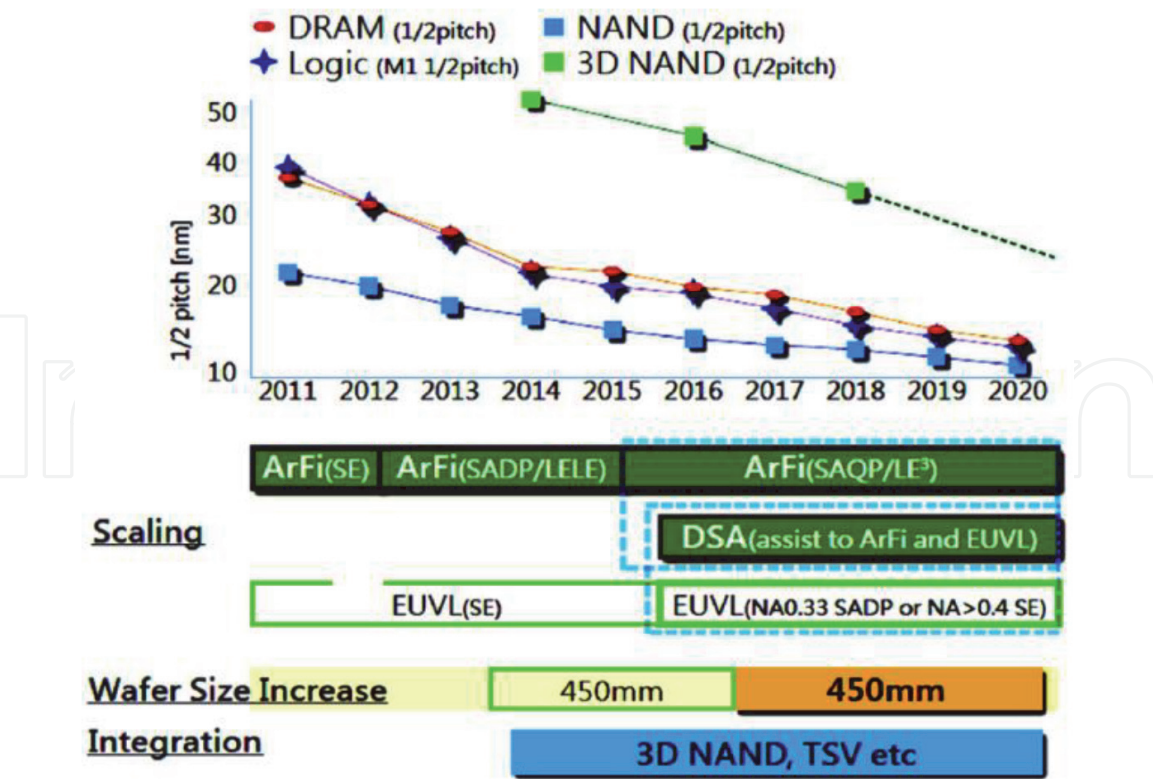


Figure 1. Development trend of key dimensions of wafer manufacturing in 2020.

12.01 ~ 7.01 advanced technology baseband chips, such as Qualcomm Snapdragon X50, MediaTek Helio M70, Intel XMM8000 series, Samsung Exynos 5000 series, Hisilicon Balong 5000 series, etc. This creates a potential demand for semiconductor equipment. 5G and artificial intelligence will not only bring the semiconductor equipment market back to a short term in 2020, but also support the development of the semiconductor equipment industry in the long term. The research and development organization predicts the technology trend in 2020, and the research and development of Toyo, a subsidiary of Jibang, predicts that the semiconductor industry will gradually come out of the bottom in 2020 with the continuous increase in demand for 5G, AI, automotive and other emerging applications. Among them, 5G transformative technologies are the most critical. The Industrial Intelligence Institute (MIC) of the China Resources Planning Association pointed out that this year, about 56 telecom operators in 32 countries have announced the deployment of 5G networks, of which 39 telecom operators have officially opened 5G services. It is estimated that by 2020, there will be 170 telecom providers worldwide providing 5G commercial services [5, 6].

Combining the foregoing, in order to achieve high accuracy and high throughput, modern FAB uses a large number of high-energy processes, such as plasma, CVD, and ion implantation. This furnace is one of the important tools for semiconductor manufacturing (Figure 2). Due to the high energy, the physicochemical changes in each reactor are very complex, and it is often impossible to determine the type and concentration of the by-products produced, and the type and concentration of these by-products often change randomly. These by-products usually cause the following effects on FAB, including: (1) Incompatibility between by-products may increase the toxicity or explosiveness of the gas in the pipeline; (2) By-products may corrode the exhaust pipe or make it brittle (3) If the type and concentration of by-products cannot be determined, it is impossible to select the appropriate exhaust gas treatment equipment; (4) The currently used processing

equipment may be damaged, which may affect the processing efficiency [7–9]. As of 2020, there are already 37 semiconductor wafers FABs in Taiwan. Taking the 12-inch FAB as an example, there are about 420 various types of main process machines in a manufacturing plant with a monthly capacity of 50,000 wafers, of which about 63 are thin film process machines, photolithography process machine also has about 55, summary of Taiwan IC manufacturing FABs show in **Table 2** [10].

Treat 100,000 pieces of factory space as a large factory, that is, all machines with similar functions are only divided into a group. The layout of the machine group is planned using a typical “non-shaped” pattern (please refer **Figure 2(b)**). A FAB is divided into several rectangular blocks, and each block is called a processing area (bay). Machines in the same machine group or machines with similar functions are placed on the same bay as the principle. The bay is located on the two sides of the FAB. In the center is the among-bay goods material handling system, which is responsible for the transportation between bay and bay. Within each bay, there is also a within-bay goods material handling system, which is responsible for the machine and transport with the machine [11].

However, due to the FAB12" 7 nm stove based on the above production management requirements, the FTIR system was installed in this study, which includes (1) confirming the characteristics of harmful process exhaust gas; (2) evaluating the processing efficiency of various process equipment process exhaust; (3) Conduct a hazard exposure assessment survey during machine maintenance and repair; (4) Confirm the concentration and source of harmful gases and particles in the clean room operating environment; (5) Identify harmful substances in the pipeline. It is intelligent with the hardware system, and the IoT module is added to the original module. In this study, various process parameters and information required by FAB are continuously obtained in the 12" stove [12, 13].

Trade names	5" FAB	6" FAB	8" FAB	12" FAB
AMPI	—	1	—	—
Liteon	—	1	—	—
EPISIL	1	2	—	—
Micron	—	—	—	3 (Taichung * 1 + Hua Ya * 2)
MOSEL	—	1	—	—
MXIC 2	—	1	1	1 (Hsinchu Science Park)
NanYa	—	—	1	1 (Taishan Nanlin Park)
PSC	—	—	—	3 (Hsinchu Science Park)
Maxchip	—	—	1	—
TSMC	—	1	7	5 (Hsinchu Science Park *3 + Tainan Science Park*2)
UMC	—	1	6	3 (Hsinchu Science Park)
VISC	—	—	3	—
Winbond	—	—	—	2 (Taichung Science Park +Tainan Science Park)
Win Semiconductor	—	1	—	—
Total	1	9	19	17

Explanation: — means “none.”

Table 2.
Summary of Taiwan IC manufacturing FABs.

Under this premise, in order to make the above software and hardware system intelligent, add the IoT module to the original module, so that we can continuously obtain various process parameters and information required by FAB in the 12" furnace process tool. Through 24 hr of continuous Processing and thousands of processing machines, we will obtain a large amount of data to confirm the above production requirements, so that we can effectively master the FAB characteristics, improve production efficiency, improve product yield and establish a safe and healthy product line and employee working environment It is an important contribution of this research [14–16].

2. Methodology and study procedure

2.1 RFID and IoT technology

The core of the FTIR is the Michealson interferometer. Its principle is that the two infrared beams after the infrared light source is split by the beam splitter are respectively directed to the fixed mirror and the moving mirror, and then combined into A single infrared ray, due to the difference in optical path formed by the moving mirror, makes the final combined infrared ray form an infrared beam of different energy due to destructive and constructive interference. It has a fast analysis speed, is not destructive to the sample, and can analyze solid liquid and gas samples, making it gradually become an indispensable qualitative tool for material analysis. In certain circumstances, it can even achieve the ability to quickly screen quantitative [17].

The instrument used in this study is aspirated FTIR. The pumped FTIR uses a pump to introduce the gas to be tested into the FTIR detection chamber for immediate analysis. The measurement method is shown in **Figure 3**. The main components of the pumped FTIR include infrared sources, interferometers, beam splitters, fixed mirrors, moving mirrors and gas chambers, detectors and electronic modules, etc. In addition, there must be a sampling tube and pump and other gas samples into the closed cavity In addition to the computer used for data collection and data analysis and appropriate software, this study also added an IoT module to the existing FTIR, allowing the FTIR to transmit and calculate. With the cloud, pumped FTIR's the instrument configuration is shown in **Figure 4** [18, 19]. For IoT part, this study starts with the sensor, imports the sensing signal into the electronic module, and exports the signal to the cloud system through the WiFi module, in this way, this study obtain FTIR sensing data 24 hr, and this system is set to obtain data once per second.

The basic design of the infrared spectrometer is to emit a beam of light to the measurement area and measure the amount of intensity change after the beam passes through the gas to be tested. Since each gas molecule has its specific infrared light absorption coefficient, when a light beam passes through the measurement region, a specific gas molecule absorbs light of a specific wavelength, so that the

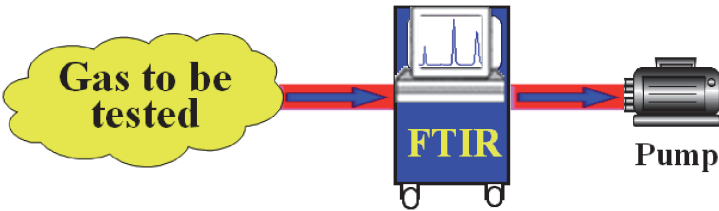


Figure 3.
Schematic diagram of instrument configuration of gas-type FTIR spectrometer.

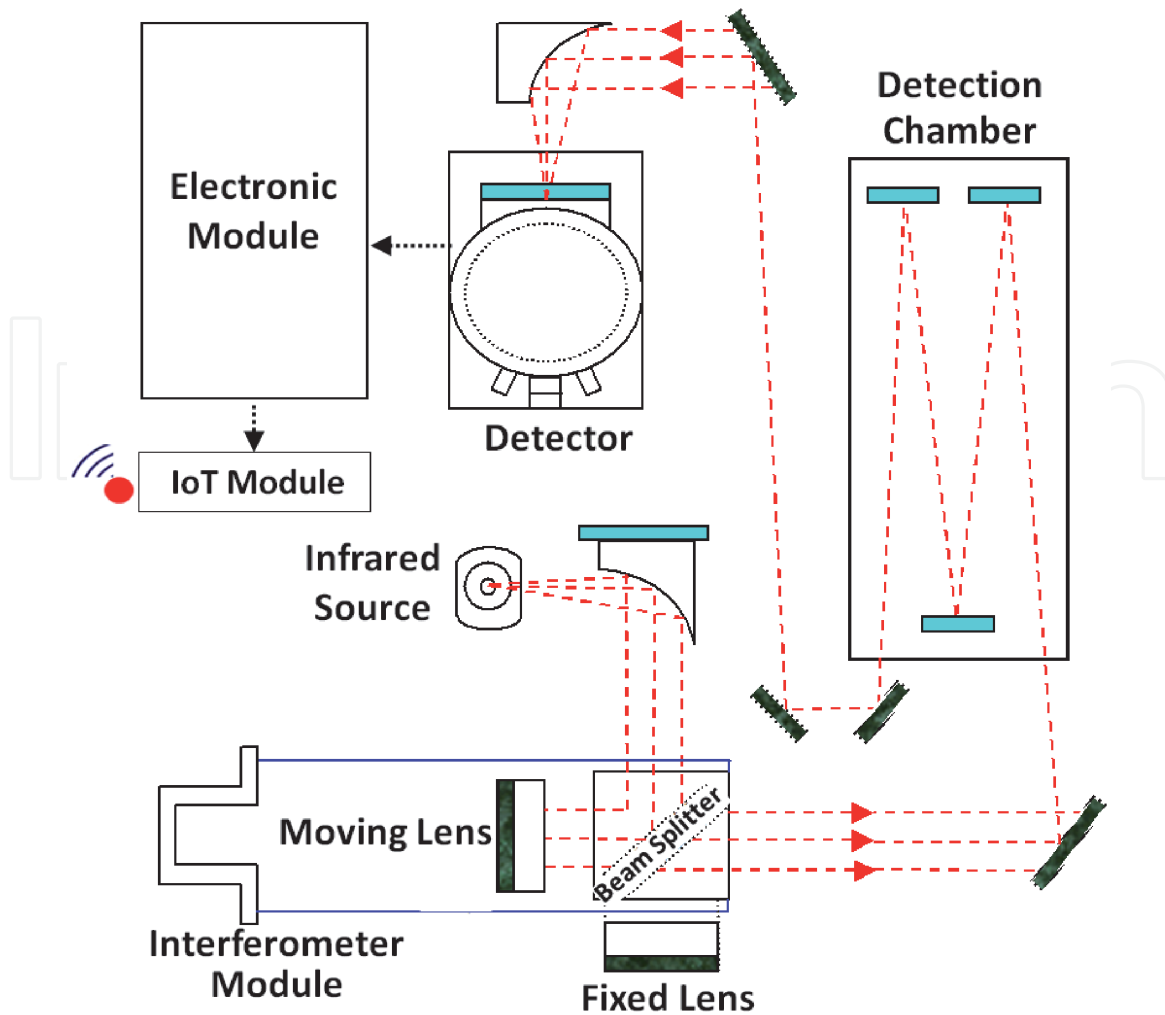


Figure 4.
The instrument configuration of the pumped FTIR.

intensity of the light beam in this wavelength band is weakened, and the ratio of light intensity before and after absorption is The concentration of the gas is directly related. The absorption band and intensity of the gas sample can be measured to know the composition and concentration contained in the gas. For a maximum path difference d adjacent wavelengths λ_1 and λ_2 will have n and $(n + 1)$ cycles respectively in the interferogram. The corresponding frequencies are ν_1 and ν_2 , and the membership function in the following Eqs. (1)~(5) [20, 21]:

$$d = n\lambda_1 \text{ and } d = (n + 1)\lambda_2 \quad (1)$$

$$\lambda_1 = d/n \text{ and } \lambda_2 = d/(n + 1) \quad (2)$$

$$\nu_1 = 1/\lambda_1 \text{ and } \nu_2 = 1/\lambda_2 \quad (3)$$

$$\nu_1 = n/d \text{ and } \nu_2 = (n + 1)/d \quad (4)$$

$$\nu_2 - \nu_1 = 1/d \quad (5)$$

FTIR mainly emits a beam of light to the measurement area and measures the intensity change of the beam after passing the gas to be measured. Since each gas molecule has its specific infrared light absorption coefficient, when the light beam passes through the measurement area, the specific gas molecule will absorb light of a specific wavelength, so that the intensity of the light beam in this band is reduced, and the ratio of the light intensity before and after absorption The concentration of the gas is directly related, and the absorption band and intensity of the gas sample

can be calculated to know the composition and concentration of the gas. **Figure 5** shows the absorption spectrum of several gas molecules in the infrared range.

2.2 Cloud system and big data analysis technology

This research is based on the fact that FTIR operates continuously for 24 hr and captures signals every second to obtain data throughout the year as a basis for big data. The main research significance is not to grasp the huge data information, but to professionally process these meaningful data, so that FAB factory managers can know whether the exhaust emissions meet the alert or warning potential under the sensing trend. Most of the research uses the big data platform for deployment, debugging and maintenance. This study is connected to the Chief Cloud eXchange (CCX) cloud database platform and the Spark big data platform. At the same time, these two platforms are also more suitable for primary systems to implement systems. **Figure 6** is the research cloud computing system and database architecture.

For the big data of the chip process exhaust obtained by RFID, full consideration should be given to (1) big data life cycle, (2) big data technology ecology, (3) big data acquisition and preprocessing, (4) big data storage and management, (5) Big data computing model and system.

The big data analysis method used in this study is described as follows. U is defined as the non-empty initial universe of the object. Then define E as a set of parameters related to the object in U . Let $P(U)$ be the power set of U , and $A \subset E$. A pair (F, A) is called a soft set on U , where F is the mapping given by a $F: A \rightarrow (U)$. In other words, the soft set on U is a parameterized family of Universe U subsets.

In addition, if the universe set U is a non-empty finite set, and σ is the equivalent relationship on U . Then (U, σ) is called approximate space. If X is a subset of U , then X can be written as a union of equivalent classes of U or not. If X can be written as a union of equivalent classes of U , then X is definable, otherwise it is undefinable. If X is undefinable, it can be approximated as two definable subsets, called the upper and lower approximation of X , as shown below Eq. (6) [22, 23].

$$\begin{aligned} \underline{app}(X) &= \cup \{ [\chi]_{\sigma} : [\chi]_{\sigma} \subseteq X \}, \\ \overline{app}(X) &= \cup \{ [\chi]_{\sigma} : [\chi]_{\sigma} \cap X \neq \emptyset \}. \end{aligned} \tag{6}$$

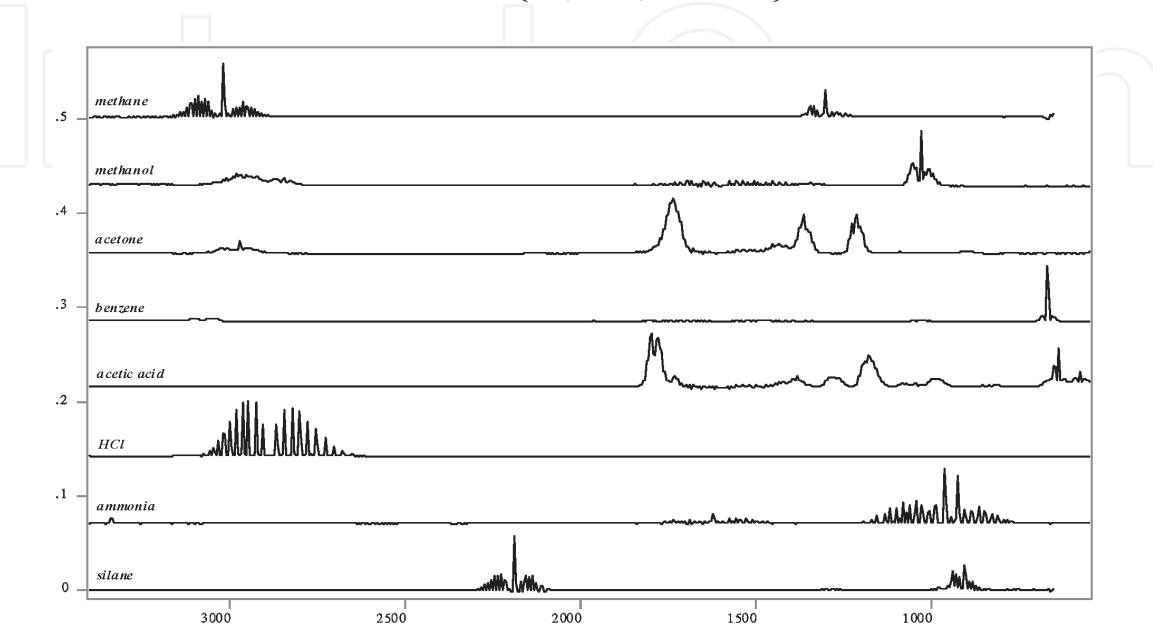


Figure 5.
The absorption spectrum of several gas molecules in the infrared range.

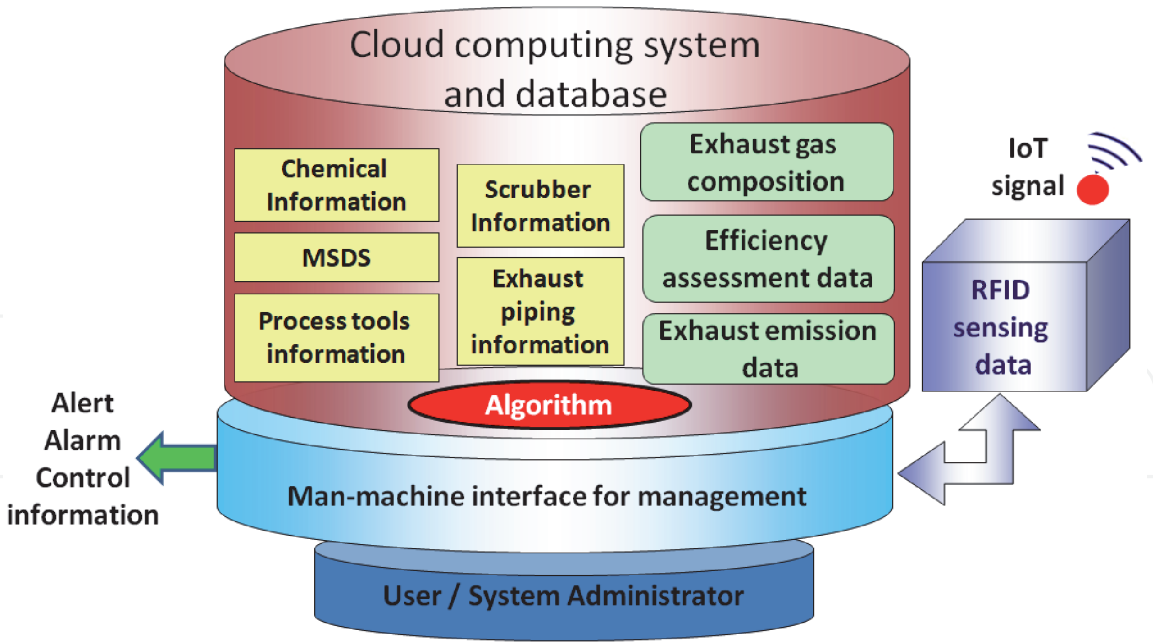


Figure 6.
The research cloud computing system and database architecture.

The process of data decomposition is defined as follows: Let X is defined as the number of groups and Y as several data, as shown below Eqs. (7)~(8).

$$X = (Y/10,000) \tag{7}$$

If X contains remainder, then

$$X = X + 1 \tag{8}$$

Where the number of groups will be added to 1.

Algorithm (1): The most optimized attribute set searching algorithm.

Input: Optimized reduct sets, R_1 until R_n Output: The most optimal reduct set.

if Reduct set R has more than one value then.

Select the highest number of attribute values, HR if HR does not have the same number with attribute value AND HR has more than one value then.

Select the first reduction set, FR of attribute values.

else

Proceed to the next process

else

Proceed to the next process

Algorithm (2): Soft set parameter reduction algorithm.

In tabular representation, let (F, P) represent the soft set. If Q is the reduction of P , the soft set reduction set is defined as (F, Q) of the soft set (F, P) where $P \subset E$.

Input: A soft set (F, E) , set P .

Output: Optimal decision.

Input the set P of choice parameters.

Find all reducts of (F, P) .

Select one reduct set (F, Q) of (F, P) .

Find weighted table of soft set (F, Q) according to the decided weights.

Find k , for which $c_k = \max c_i$.

h_k is the optimal choice of value for the selected object. If k has more than one value, any one of the benefits could be chosen.

c_i is the choice of value of an object h_i where $c_i = \sum_j h_{ij}$ and h_{ij} is the entries in the table of the reduct soft set.

Algorithm (3): Rough set parameter reduction algorithm.

Input: An information system $S = (U, A, V, f)$.

U is a finite nonempty set object.

A is a finite nonempty set of attributes.

V is a nonempty set of values.

f is an information function that maps an object in U to exactly one value in V .

Output: Simplified reduct sets.

Input the information Table S .

Discretization of data.

Forming up the $n \times n$ discernibility matrix. The elements of S table is defined as $d(x, y) = a \in A \mid f(x, a) \neq f(y, a)$, $d(x, y)$ is an attribute.

set distinguishing x and y . For each attribute $a \in A$, if $d(x, y) = a_1, a_2, \dots, a_k \neq \emptyset$.

Formulate the Boolean function $a_1 \vee a_2 \dots \vee a_k$ or discernibility function which represented by $\sum d(x, y)$ as indicated: $F(A) = \prod_{(x,y) \in U \times U} \sum d(x, y)$.

If $d(x, y) = \emptyset$, constant 1 will be assigned to the Boolean function.

Execute the attribute reduction process based on the simplified Boolean function.

New optimized reduct sets are generated.

2.3 Process design and discussion

In the reactor, chemical reaction is used to form the reactant (usually a gas) into a solid product, and a thin film is deposited on the surface of the wafer. This process is called CVD (Chemical Vapor Deposition). This process has (1) good step coverage, (2) energy with high aspect ratio gap filling, (3) good thickness uniformity, (4) high pure and dense, (5) when ratio can be controlled, (6) low stress for high film quality, (7) good electrical properties, (8) base plate and excellent film adhesion characteristics. **Figure 7** shows the system architecture of CVD in FAB.

The precipitation of products during the CVD process can be divided into the following steps: (1) the source gas diffuses to the substrate surface, (2) the substrate adsorbs the source gas, (3) the substances adsorbed on the substrate react chemically on its surface, (4) The precipitated material diffuses on the surface of the substrate, (5) The reaction product is separated from the gas-phase reactant, (6) The precipitated non-volatile material is deposited on the substrate surface by diffusion and the like. The composition, structure and performance of the products obtained in this chemical reaction can be controlled by changing the parameters of the reaction. The reaction parameters mainly include the type of gas, the gas reaction concentration, the delivery method of the reactant, the gas flow rate, the total gas pressure and the Area pressure, heating method, substrate material, substrate surface state, substrate reaction temperature, temperature distribution and gradient, etc.

When entering the 7-nanometer process, the channel material of the semiconductor PN junction must also be changed. Since the electron mobility of silicon is $1500 \text{ cm}^2 / \text{Vs}$, and germanium can reach $3900 \text{ cm}^2 / \text{Vs}$, and the implementation

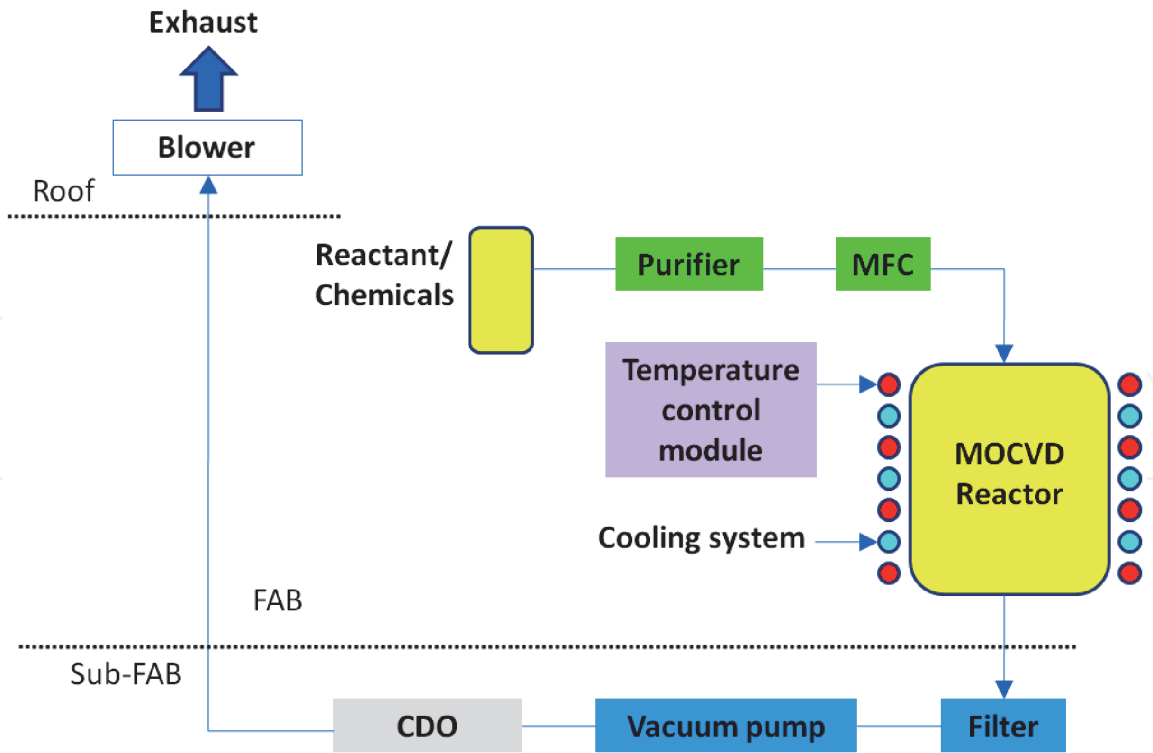


Figure 7.
The system architecture of CVD in FAB.

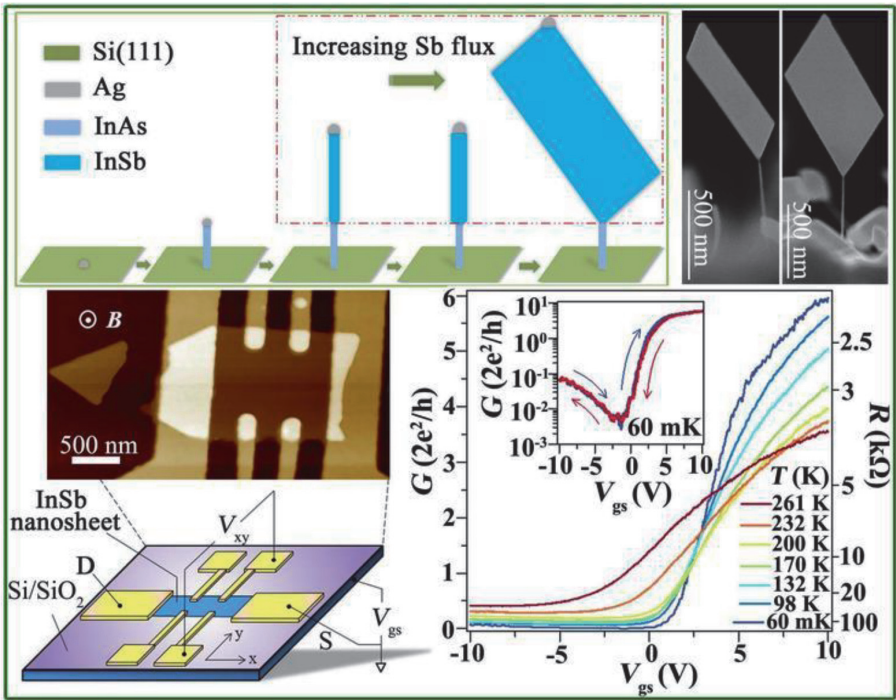


Figure 8.
7 nm process device structure and characteristics.

voltage of silicon devices is 0.75 ~ 0.8 V, while the germanium devices are only 0.5 V, so germanium was Considered to be the preferred material for MOSFET transistors, the first 7-nanometer wafer in IBM Lab used Ge-Si material. IMEC researched new germanium-doped materials and screened two channel materials that can be used for 7 nm: one is PFET composed of 80% germanium and the other is 25 ~ 50% mixed germanium FET Or 0 ~ 25% NFET mixed with germanium (**Figure 8**) [24, 25].

characteristic	LP-TEOS	PE-TEOS	AP-TEOS/O ₃
Deposition temperature (°C)	650 ~ 750	300 ~ 400	350 ~ 450
Operating pressure (Torr)	1 ~ 10	0.1 ~ 5	500 ~ 700
Sedimentary composition	SiO ₂	SiO ₂ :H	SiO ₂
Density(g/cm ³)	2.2	2.3	2.15
Refractive index	1.43 ~ 1.46	1.47 ~ 1.5	1.45
Dielectric constant	4.0	4.1 ~ 4.9	4.4
BOE(100:1) Etching rate ()	30	400	1200
Stress value (dyne/cm ²)	1 ~ 3 × 10 ⁹	-(1 ~ 5 × 10 ⁹)	10 ⁸ ~ 3 × 10 ⁹

Table 3.
Summary of process parameters and characteristics of TEOS.

Air pollutants	Equipment efficiency standard	Total control standards
Volatile Organic Compounds	>90%	<0.6 kg/hr (calculated based on methane)
Trichloroethylene	>90%	<0.02 kg/hr
Nitric acid, hydrochloric acid, phosphoric acid and hydrofluoric acid	>95%	<0.6 kg/hr
Sulfuric acid droplets	>95%	<0.1 kg/hr

Table 4.
Standards of FAB total emissions.

The silicon dioxide in the device, in this study, uses TEOS as the raw material, Tetraethyl Orthosilicate, the chemical formula is Si (OC₂H₅)₄. High boiling point (about 169° C under normal pressure), store and use in liquid form. TEOS is liquid at room temperature and normal pressure. In order to increase the use of CVD process and the stability of the process, the TEOS container (about 40 ~ 70°C) is heated during use to increase its saturated vapor pressure In the gaseous use of TEOS in the deposition reaction of CVD. The process parameters and characteristics of TEOS are summarized in **Table 3**.

According to the “Semiconductor Manufacturing Air Pollution Control and Emission Standards” announced by the Environmental Protection Agency of the Taiwan Government, air pollutants produced in the process should be discharged after being purified by the appropriate system, where the efficiency of the system or the total emissions of the entire factory should be Meet the standards listed in the **Table 4**.

3. FTIR sensing system of IoT and experiment settings

In order to achieve high precision and high output, modern high-energy processes such as plasma are important tools for semiconductor manufacturing. The physicochemical changes that occur in each reactor due to high energy are quite complicated, and the type and concentration of by-products cannot often be determined. These by-products usually have the following effects on the plant. (1) Incompatibility between by-products may increase the toxicity or explosiveness of

the gas in the pipeline; (2) By-products may cause corrosion or embrittlement of exhaust pipe materials; (3) If the type and concentration of by-products cannot be determined, appropriate exhaust gas treatment equipment may be selected; (4) damage may be caused to the currently used treatment equipment, which may affect treatment efficiency. Based on the aforementioned production management requirements, the 12" furnace FTIR system installed by FAB includes (1) confirmation of the characteristics of hazardous process exhaust gas; (2) evaluation of the processing efficiency of various process exhaust gas treatment equipment; (3) investigation of hazardous sources. Condition assessment during machine maintenance and repair; (4) Confirm the concentration and source of harmful gases and particulate matter in the clean room operating environment [26–28].

In this study, open-path FTIR was used to monitor the air quality of clean room to ensure the air quality of the working environment and the health of employees.

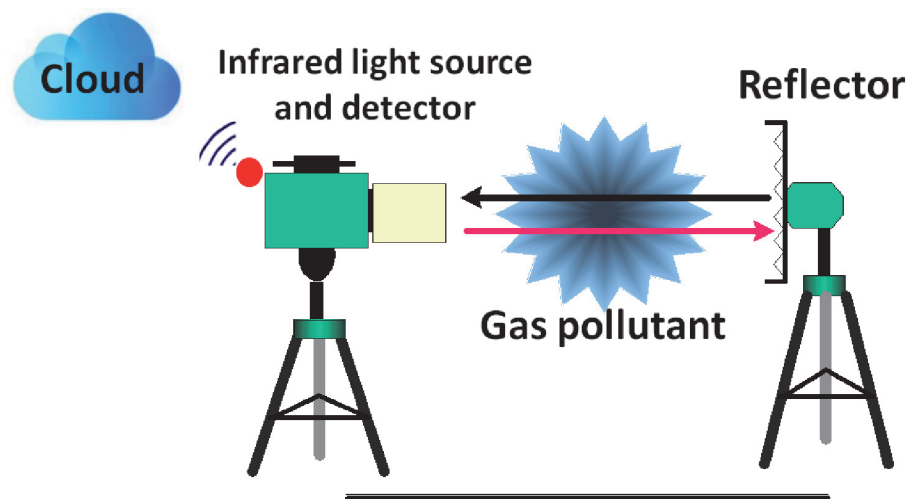


Figure 9.
The FTIR field setting architecture.

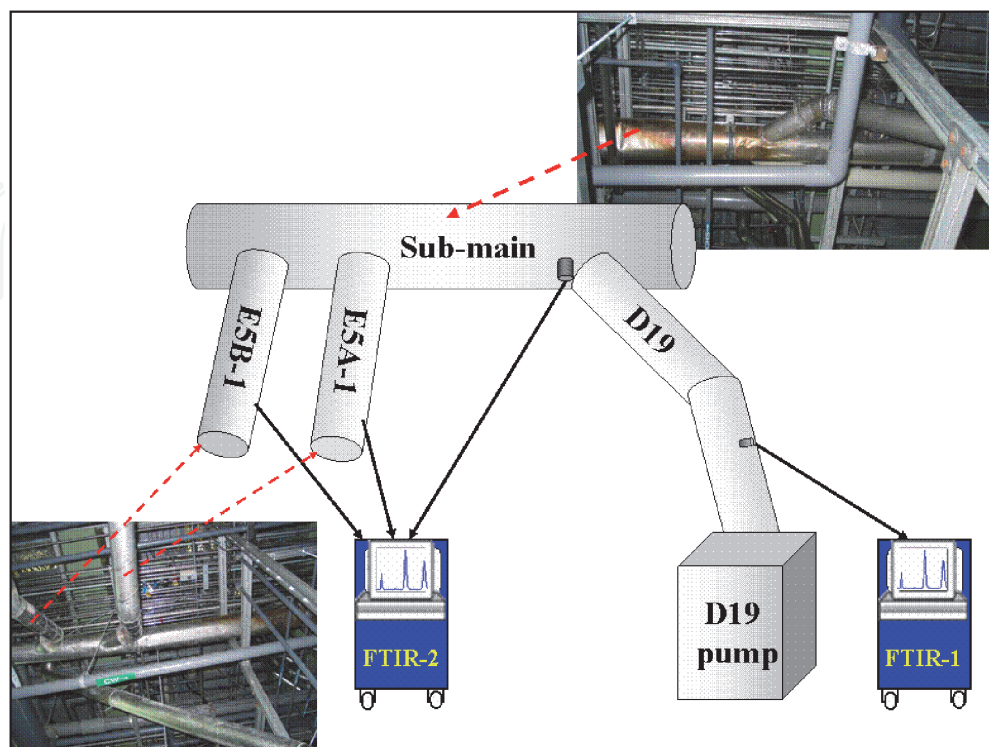


Figure 10.
This study was set on the site to set the exhaust line of the furnace control process.

This study set up two measuring points in the 12" factory of Hsinchu Science Park in Taiwan, as shown in **Figure 11**. **Table 5** shows the process parameters of the on-site process tools during our experiment, and **Table 6** shows the processing parameters of the on-site machine exhaust gas treatment equipment. Among them, Inlet flow rate (Q_i) estimated from the TEOS injection = 89 LPM, Initial outlet flow rate (Q_o) estimated from the TEOS injection = 292 LPM. Therefore, dilution ratio = $Q_o/Q_i = 292/89 = 3.3$.

4. FTIR IoT experiment result and big data analysis

From the measurement data of this study, it can be found (**Figure 12**) that the main reactant of the thin film process is TEOS for BPSG, so almost all reactions are carried out in the reaction chamber, or become a composite, which does not exist in

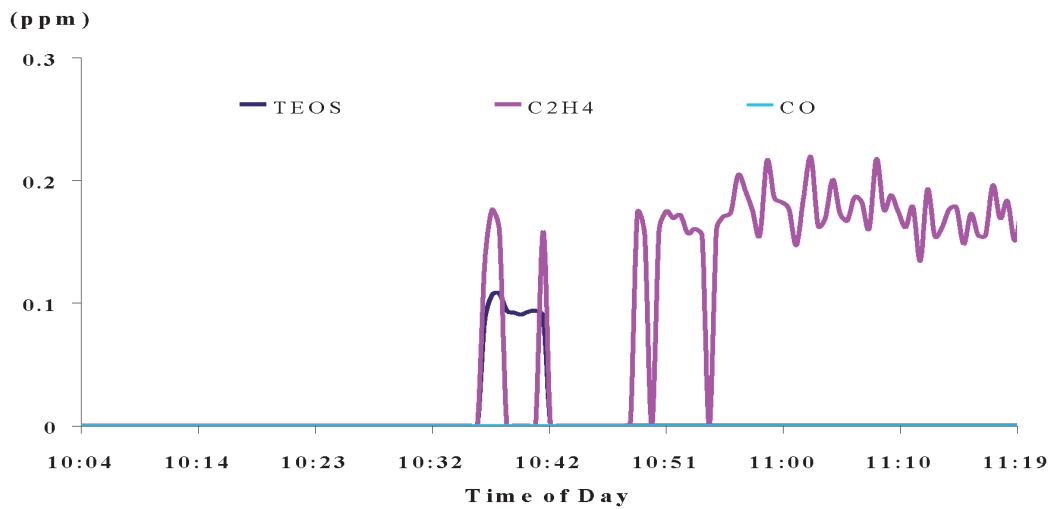


Figure 12.
Main exhaust pipe concentration trend (A point).

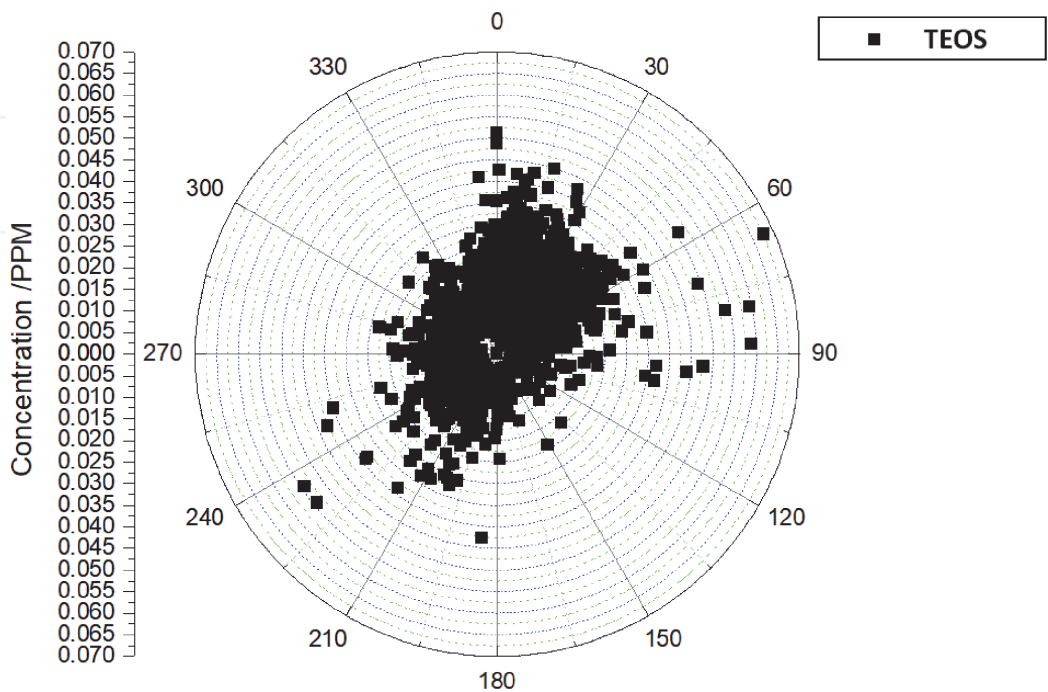


Figure 13.
Results of scatter diagram for calculation of concentration distribution for one consecutive year (A point).

the main exhaust gas pipeline, the beginning of the reaction concentration between 0.08 ~ 0.1 ppm only. C₂H₄ is mainly used for cleaning the reaction chamber, concentration between 0.15 ~ 0.25 ppm. Therefore, when the main process is carried out, the high concentration of the input will be cleaned, so the high concentration state can be seen in the main exhaust pipe. On the other hand, the CO is active because it is in the process of production, so it is difficult to find the concentration of the main exhaust pipe. **Figures 13 and 14** are the results of the study after optimizing the concentration values measured at the day of point A.

Figure 15 shows secondary main exhaust pipe concentration trend. Due to the proximity of the process chamber, the concentrations are clearly detected, especially CO is more obvious, concentration between 1 ~ 1.7 ppm, and TEOS is liquid because it is normal and concentration between 0.4 ~ 0.6 ppm, so although the concentration near the reaction chamber is high, condensation occurs when entering the low temperature zone, so only this The section pipeline is measured, and the main exhaust pipe is not obvious. The C₂H₄ concentration is between 1.5 ~ 2.0 ppm.

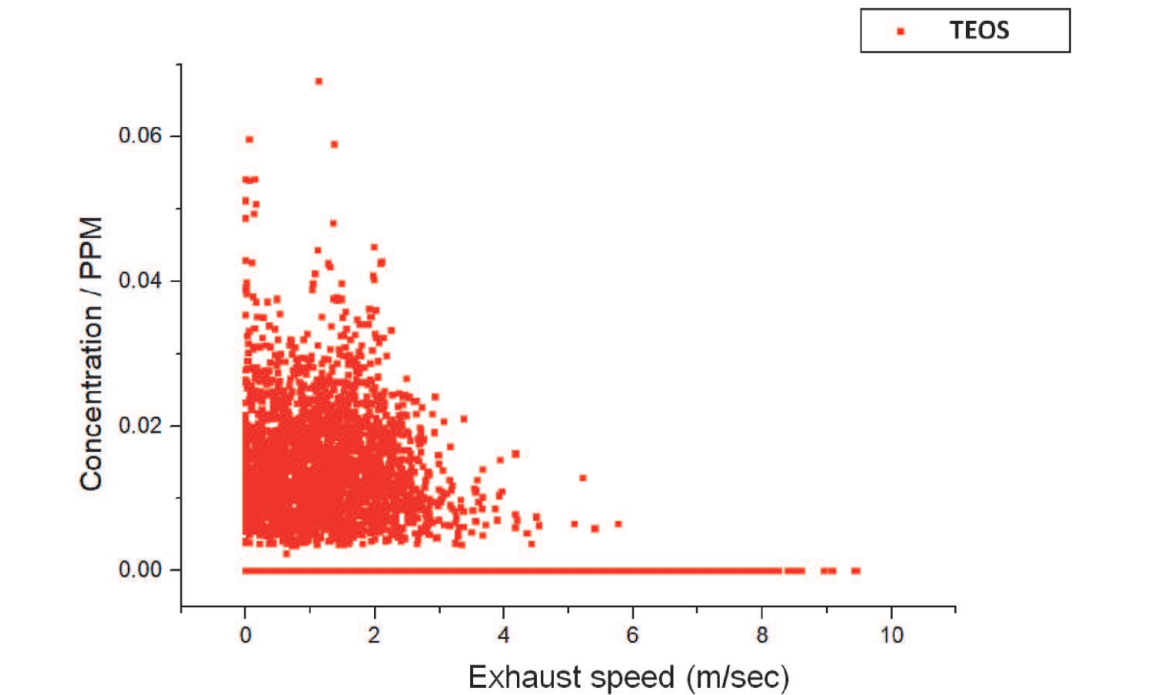


Figure 14.
Achievement of the calculation of the concentration value distribution for one consecutive year (A point).

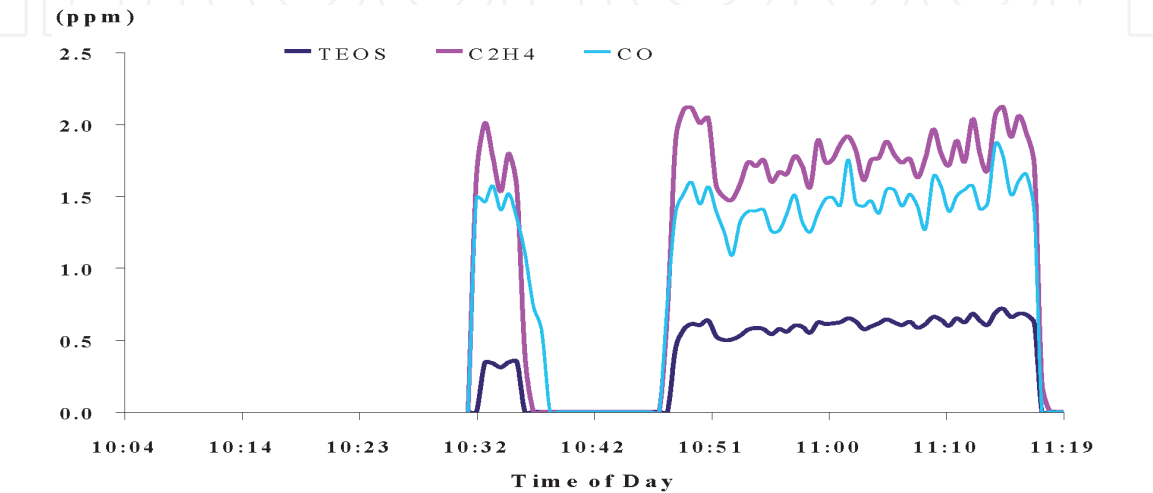


Figure 15.
Secondary main exhaust pipe concentration trend (B point).

According to the OSHA regulations, this study is set in the cloud database for big data analysis and decision making, when the upper limit of TEOS, C_2H_4 , CO are 0.6, 2.0, 1.7 ppm; the lower limit of TEOS, C_2H_4 , CO is 0.4, 1.5, 1 ppm. The application architecture of this study can be extended to other semiconductor processes, so that IoT integration and big data operations can be performed for all processes, this is an important step in promoting FAB intelligent production and an important contribution of this study.

5. Conclusion and suggestion

In order to achieve high precision and yield, modern FABs use a large number of high-energy processes such as plasma, CVD and ion implantation, the furnace is one of the important tools of semiconductor manufacturing. The FAB installed FTIR system due to the 12" furnace tools based on the aforementioned production management requirements. The principle of measurement is the same as the principle of Extractive FTIR, but the closed cavity is changed to open type and integrated IoT mechanism to connect to the cloud, which is suitable for a variety of gaseous pollutants (including organic gases and inorganic gaseous pollutants) in the atmosphere are monitored in this study. This study set up two measuring points of furnace process tools in the 12" factory of Hsinchu Science Park in Taiwan. This study obtained FTIR measurements, and according to the OSHA regulations, this study is set in the cloud database for big data analysis and decision making, when the upper limit of TEOS, C_2H_4 , CO are 0.6, 2.0, 1.7 ppm; the lower limit of TEOS, C_2H_4 , CO is 0.4, 1.5, 1 ppm. The application architecture of this study can be extended to other semiconductor processes, so that IoT integration and big data operations can be performed for all processes, this is an important step in promoting FAB intelligent production and an important contribution of this study.

IntechOpen

Author details

Kuo-Chi Chang^{1,2*}, Kai-Chun Chu¹, Hsiao-Chuan Wang³, Yuh-Chung Lin¹,
Tsui-Lien Hsu⁴ and Yu-Wen Zhou¹

¹ Fujian University of Technology, China

² College of Mechanical and Electrical Engineering, National Taipei University of
Technology, Taiwan

³ Institute of Environmental Engineering, National Taiwan University, Taiwan

⁴ Institute of Construction Engineering and Management, National Central
University, Taiwan

*Address all correspondence to: albertchangxuite@gmail.com

IntechOpen

© 2020 The Author(s). Licensee IntechOpen. This chapter is distributed under the terms of the Creative Commons Attribution License (<http://creativecommons.org/licenses/by/3.0>), which permits unrestricted use, distribution, and reproduction in any medium, provided the original work is properly cited. 

References

- [1] Lu CC, Chang KC, Chen CY. Study of high-tech process furnace using inherently safer design strategies (IV). The advanced thin film manufacturing process design and adjustment. *Journal of Loss Prevention in the Process Industries*. 2016;**40**:378-395
- [2] Chen C-Y, Chang K-C, Wang G-B. Study of high-tech process furnace using inherently safer design strategies (I) temperature distribution model and process effect. *Journal of Loss Prevention in the Process Industries*. 2013;**26**(6):1198-1211, ISSN 0950-4230. DOI: 10.1016/j.jlp.2013.05.006
- [3] Lu CC, Chang KC, Chen CY. Study of high-tech process furnace using inherently safer design strategies (III) advanced thin film process and reduction of power consumption control. *Journal of Loss Prevention in the Process Industries*. 2016;**43**:280-291
- [4] Chen C-Y, Chang K-C, Lu C-C, Wang G-B. Study of high-tech process furnace using inherently safer design strategies (II). Deposited film thickness model. *Journal of Loss Prevention in the Process Industries*. 2013;**26**(1):225-235, ISSN 0950-4230. DOI: 10.1016/j.jlp.2012.11.004
- [5] Chang KC, Chu KC, Wang HC, Lin YC, Pan JS. Energy saving technology of 5G base station based on internet of things collaborative control. *IEEE Access*. 2020;**8**:32935-32946
- [6] Li S, Da Xu L, Zhao S. 5G internet of things: A survey. *Journal of Industrial Information Integration*. 2018;**10**:1-9, ISSN 2452-414X. DOI: 10.1016/j.jii.2018.01.005
- [7] Sze SM, Ng KK. *Physics of Semiconductor Devices*. 3rd ed. Canada: Wiley; 2006. ISBN: 978-0-471-14323-9
- [8] Chang K-C, Lin Y-C, Chu K-C. Mobile edge computing technology and local shunt design. *The Frontiers of Society, Science and Technology*. 2019; **1**(10):135-140. DOI: 10.25236/FSST.2019.011017
- [9] Chen C-Y, Chang K-C, Huang C-H, Lu C-C. Study of chemical supply system of high-tech process using inherently safer design strategies in Taiwan. *Journal of Loss Prevention in the Process Industries*. 2014;**29**:72-84, ISSN: 0950-4230. DOI: 10.1016/j.jlp.2014.01.004
- [10] Zhou YW et al. Study on IoT and big data analysis of furnace process exhaust gas leakage. In: Pan JS, Li J, Tsai PW, Jain L, editors. *Advances in Intelligent Information Hiding and Multimedia Signal Processing. Smart Innovation, Systems and Technologies*. Vol 156. Singapore: Springer; 2020
- [11] Chang KC, Chu KC, Chen T, Lee YW, Lin YC, Nguyen T. Study of the high-tech process mechanical integrity and electrical safety. In: 14th International Microsystems, Packaging, Assembly and Circuits Technology Conference (IMPACT). Taipei, Taiwan: IEEE; 2019. pp. 162-165
- [12] Chang KC, Chu KC, Horng D, Lin JC, Yi-Chun Chen V. Study of wafer cleaning process safety using inherently safer design strategies. In: 2018 13th International Microsystems, Packaging, Assembly and Circuits Technology Conference (IMPACT). Taipei, Taiwan: IEEE; 2018. pp. 218-221
- [13] Loke ALS et al. Analog/mixed-signal design challenges in 7-nm CMOS and beyond. In: 2018 IEEE Custom Integrated Circuits Conference (CICC). San Diego, CA: IEEE; 2018. pp. 1-8
- [14] Khan MA, Salah K. IoT security: Review, blockchain solutions, and open challenges. *Future Generation Computer Systems*. 2018;**82**:395-411. ISSN: 0167-739X. DOI: 10.1016/j.future.2017.11.022

- [15] Chang K-C, Chu K-C, Wang H-C, Lin Y-C, Pan J-S. Agent-based middleware framework using distributed CPS for improving resource utilization in smart city. *Future Generation Computer Systems*. 2020; **108**:445-453. ISSN 0167-739X. DOI: 10.1016/j.future.2020.03.006
- [16] Novo O. Blockchain meets IoT: An architecture for scalable access management in IoT. *IEEE Internet of Things Journal*. 2018;5(2):1184-1195
- [17] Müsellim E, Tahir MH, Ahmad MS, Ceylan S. Thermokinetic and TG/DSC-FTIR study of pea waste biomass pyrolysis. *Applied Thermal Engineering*. 2018;137:54-61. ISSN: 1359-4311. DOI: 10.1016/j.applthermaleng.2018.03.050
- [18] Huang M, Li Z, Huang B, Luo N, Zhang Q, Zhai X, et al. Investigating binding characteristics of cadmium and copper to DOM derived from compost and rice straw using EEM-PARAFAC combined with two-dimensional FTIR correlation analyses. *Journal of Hazardous Materials*. 2018;344:539-548. ISSN: 0304-3894. DOI: 10.1016/j.jhazmat.2017.10.022
- [19] Petit T, Puskar L. FTIR spectroscopy of nanodiamonds: Methods and interpretation. *Diamond and Related Materials*. 2018;89:52-66. ISSN: 0925-9635. DOI: 10.1016/j.diamond.2018.08.005
- [20] Amesimenu DK et al. Home appliances control using android and arduino via bluetooth and GSM control. In: Hassanien AE, Azar A, Gaber T, Oliva D, Tolba F, editors. *Proceedings of the International Conference on Artificial Intelligence and Computer Vision (AICV2020)*. AICV 2020. *Advances in Intelligent Systems and Computing*. Vol 1153. Cham: Springer; 2020
- [21] Primpke S, Wirth M, Lorenz C, et al. Reference database design for the automated analysis of microplastic samples based on Fourier transform infrared (FTIR) spectroscopy. *Analytical and Bioanalytical Chemistry*. 2018;410:5131-5141. DOI: 10.1007/s00216-018-1156-x
- [22] Mohamad M, Selamat A, Krejcar O, Fujita H, Wu T. An analysis on new hybrid parameter selection model performance over big data set. *Knowledge-Based Systems*. 2020;192:105441. ISSN: 0950-7051. DOI: 10.1016/j.knosys.2019.105441
- [23] Tao F, Cheng J, Qi Q, et al. Digital twin-driven product design, manufacturing and service with big data. *International Journal of Advanced Manufacturing Technology*. 2018;94:3563-3576. DOI: 10.1007/s00170-017-0233-1
- [24] Jang D et al. Self-heating on bulk FinFET from 14nm down to 7 nm node. In: 2015 IEEE International Electron Devices Meeting (IEDM). Washington, DC: IEEE; 2015. pp. 11.6.1-11.6.4
- [25] Tian H, Chang K-C, Chen JS. Application of hyperbolic partial differential equations in global optimal scheduling of UAV. *Alexandria Engineering Journal*. 2020. DOI: 10.1016/j.aej.2020.02.013 [Available online 21 February 2020, in press]
- [26] Chang KC et al. Study on hazardous scenario analysis of high-tech facilities and emergency response mechanism of science and technology parks based on IoT. In: Pan JS, Lin JW, Liang Y, Chu SC, editors. *Genetic and Evolutionary Computing. ICGEC 2019. Advances in Intelligent Systems and Computing*. Vol. 1107. Singapore: Springer; 2020
- [27] Chang KC, Chu KC, Lin YC, Nguyen T, Pan J. Study of inherently safer design strategy application for IC process power supply system. In: 14th International Microsystems, Packaging, Assembly and Circuits Technology

Conference (IMPACT). Vol. 2019.
Taipei, Taiwan: IEEE; 2019. pp. 158-161

[28] Chu KC, Horng DC, Chang KC.
Numerical optimization of the energy
consumption for wireless sensor
networks based on an improved ant
colony algorithm. IEEE Access. 2019;7:
105562-105571

IntechOpen

IntechOpen